MECHANICAL WORK REDUCTION DURING MANIPULATION TASKS OF A PLANAR 3-DOF MANIPULATOR

DAN N. DUMITRIU[1,2], THIEN VAN NGUYEN[2], ION STROE[2], MIHAI MĂRGĂRITESCU[3]

Abstract. The problem addressed in this paper concerns a planar 3-DOF manipulator operating in horizontal plane, that must move from an initial position characterized by angles $\theta_1(0)$, $\theta_2(0)$ and $\theta_3(0)$ to a required final position characterized by angles $\theta_1(T_F)$, $\theta_2(T_F)$ and $\theta_3(T_F)$. The manipulator can follow any trajectory from the initial to the final position, the goal being to reduce as much as possible the overall mechanical work of this manipulation task in horizontal plane. The approach here is not an optimal theory one, so that to find the global minimum of the overall mechanical work function. Our proposal is just a simple engineering method to reduce the overall mechanical work, trying several possibilities of simple methods of trajectory generation: (1) variations of θ_i parameters corresponding to constant accelerations a^+_i from $t_0 = 0$ to $t_{1/2} = T_F/2$, followed by constant decelerations $a^-_i = -a^+_i$ from $t_{1/2} = T_F/2$ to T_F; (2) variations/evolutions of θ_i parameters having the form of cosine functions; (3) evolutions of θ_i parameters corresponding to straight line variations, but using smooth departures at t_0 and smooth arrivals at T_F, with limitations concerning the departure accelerations and arrival decelerations; (4) considering the evolutions of angles $\theta_1(t)$, $\theta_2(t)$ and $\theta_3(t)$ between the initial time $t_0 = 0$ and the final time T_F, as linear segments between $t_0 = 0$ and $t_{1/2} = T_F/2$ on one hand, and as other linear segments between $t_{1/2} = T_F/2$ and T_F on the other hand. In this fourth case of trajectory, smooth departures, arrivals and transitions from one straight linear segment to another were also considered, thus limiting the maximum torques in the actuators. The results are interesting from an engineering point of view: a non-optimal minimization of the overall mechanical work is analyzed. From the point of view of protecting the actuators and thus increasing their lifetime, a second important criterion was also taken into account: the maximum torques were compared for the four possibilities of trajectories considered here. Further work will find the optimal solution of this manipulation problem, which will better evaluate the performance of the method proposed in this paper for mechanical work and maximum torque reduction.

Key words: planar 3-DOF manipulator, manipulation task, mechanical work reduction, maximum torque.

[1] Institute of Solid Mechanics of the Romanian Academy, Bucharest, Romania, e-mail: dumitri04@yahoo.com, dumitriu.dan.n@gmail.com

[2] University POLITEHNICA of Bucharest, Romania

[3] National Institute of Research and Development for Mechatronics and Measurement Technique – INCDMTM, Bucharest, Romania

Ro. J. Techn. Sci. – Appl. Mechanics, Vol. 63, N° 2, P. 165–181, Bucharest, 2018

1. PROBLEM

Since the dynamics of planar 3-DOF manipulators represents a common problem, a classical introduction comprising the state-of-art will not be detailed here. The problem will be directly presented, focusing on the issue of simple methods for identifying those trajectories that reduce the overall mechanical work of a multibody system evolving from an initial to a final desired posture.

The idea of this work started from a previous paper [1], where the end-effector of a planar 3-DOF manipulator was following a desired trajectory, with an imposed orientation of the end-effector. More precisely, a serial planar manipulator with three degrees of freedom (DOF) was simulated to perform the following task: the tip C of the end-effector followed a given curve, while the orientation of the end-effector (third element) was kept perpendicular to the followed curve. Two case studies were simulated [1]: (a) the tip C followed the straight line from point (0.25m; 0) located on ***x*** axis, to point (0; 0.25m) located on ***y*** axis; (b) the tip C of the end-effector followed a quarter of circle of radius 0.25m and having its center in (–0.10m; 0).

Figure 1 shows the planar 3-DOF manipulator used in this paper, the same as the one used in [1,2] in what concerns its model, while the inertial and geometric parameters are slightly different.

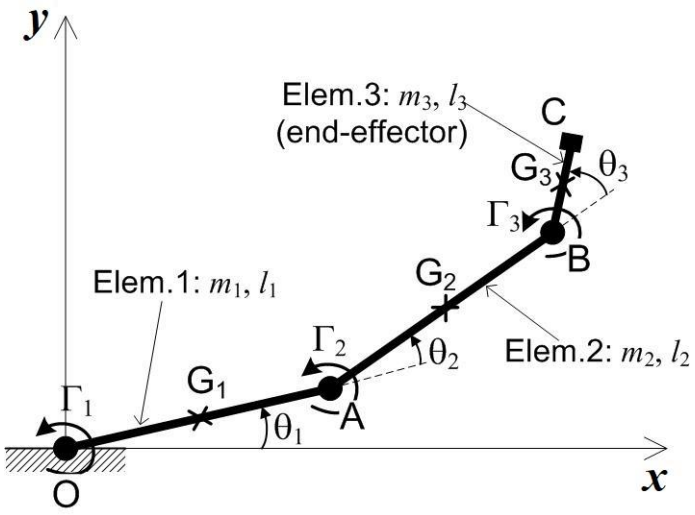

Fig. 1 – Model of the planar 3-DOF manipulator [1].

The planar 3-DOF manipulator is composed of three serial arms, each of mass m_i and length l_i (i =1,2,3). The first element/arm is articulated to the fixed frame in joint O, which is also the origin of the inertial reference frame (O, ***x***, ***y***).

The external torque Γ_1 is applied to this solid 1, in joint O. The second arm is articulated to the first element in joint A, where the external torque Γ_2 is applied, acting on this second arm. Finally, the end-effector of the manipulator (third element) is articulated to the second element/arm in joint B, being actuated by the external torque Γ_3 applied in point B. The three elements are considered as homogenous bars, having their mass center G_i (i =1,2,3) located in the middle of the bar element.

For this planar 3-DOF manipulator, inverse dynamics is performed here for the following manipulation task in the horizontal plane: the end-effector tip C must move from an initial posture (at initial time $t_0 = 0$) of the manipulator given by: $\theta_1(t_0) = -1.047197$ rad = –60°, $\theta_2(t_0) = 1.745329$ rad = 100° and $\theta_3(t_0) = -0.349066$ rad = –20°, to the required final posture given by: $\theta_1(T_F) = 1.308997$ rad = 75°, $\theta_2(T_F) = 1.047197$ rad = 60° and $\theta_3(T_F) = 0.349066$ rad = 20°. It was denoted by θ_1 the angle between $\boldsymbol{x}$ and OA, by θ_2 the angle between OA and AB and by θ_3 the angle between AB and BC. The maneuver time is $T_F = 20$ seconds.

So, the goal is to perform this manipulation task from the initial to the final position/posture, with the initial and final positions/postures characterized by null velocities. The manipulator can follow any trajectory from the initial to the final posture. The requirement is to perform this manipulation task in the horizontal plane with as less overall mechanical work consumption as possible, keeping also an eye on the maximum torques values. Obviously, this mechanical work reduction issue can be formulated as a classical nonlinear optimal/minimization problem, its numerical solution being more or less easy to find. In fact, Dumitriu et al. [3] studied such an optimal trajectory problem for a scalar 2-DOF manipulator, using a reliable hybrid method consisting of an improved dynamic programming method combined with a shooting method based on Pontryagin Maximum Principle formulation [3].

Evolved search methods such as the Genetic Algorithm (GA) can be also successfully used for the motion planning of robot manipulators [4,5]. More precisely, the GA objective function minimizes both traveling time and space, while not exceeding a maximum pre-defined torque and while ensuring obstacle avoidance, for a 3-link (redundant) robot arm. Eventually, the GA minimization can be followed by a nonlinear minimization using gradient descent methods (thus obtaining a powerful hybrid method), in order to rapidly "descend" towards the optimal solution.

So, these optimization methods are available to find the optimal trajectories, minimizing for example the overall mechanical work. But the solution is not always trivial and feasible in real-time, since the numerical solving of such nonlinear minimization problems can raise convergence difficulties, even using powerful hybrid methods.

The question is why using such problematic optimizations methods, if instead one can find solutions quite close to the optimal one (from the point of view of the considered objective function), using simple "engineering" trajectories.

Thus, the approach proposed in this paper is not an optimal theory one: as a more simplistic alternative to finding the optimal solution, our proposal is to perform just a reduction (not minimization) of the overall mechanical work function by comparing four simple engineering methods to generate trajectories:

(1) trajectory corresponding to the variation/evolution of each θ_i (i=1,2,3) by means of a constant acceleration a^+_i between $t_0 = 0$ and $t_{1/2} = T_F/2$, followed by a constant deceleration $a^-_i = -a^+_i$ from $t_{1/2} = T_F/2$ to T_F;

(2) trajectory corresponding to the variation of each θ_i (i=1,2,3) under the form of cosine functions;

(3) trajectory generated under the form of parameters θ_i (i=1,2,3) evolutions corresponding to straight line variations, but using a smooth departure at t_0 and a smooth arrival at T_F, with limitations concerning the departure acceleration and arrival deceleration;

4) trajectory obtained by considering the evolutions of angles $\theta_1(t)$, $\theta_2(t)$ and $\theta_3(t)$ between the initial time $t_0 = 0$ and the final time T_F, as linear segments between $t_0 = 0$ and $t_{1/2} = T_F/2$ on one hand, and other linear segments between $t_{1/2} = T_F/2$ and T_F on the other hand. More precisely, we consider that each θ_i (i=1,2,3) evolves from $\theta_i(t_0)$ to $\theta_i(T_F)$ by means of two simple linear segments, one segment from t_0 to $T_F/2$ and another segment from $T_F/2$ to T_F. In this fourth case of trajectory choice, smooth departures, arrivals and transitions from one straight line/segment to another were considered as well.

As mentioned, the global minimum of the overall mechanical work among all possible trajectories will not be provided by one of these four simple engineering possibilities of trajectories, but this study will draw conclusions on how to obtain trajectories quite close to the optimal trajectory.

2. DIRECT AND INVERSE DYNAMICS OF THE PLANAR 3-DOF MANIPULATOR

The direct geometric model and its inverse, the direct and inverse kinematics, as well as the direct and inverse dynamic equations written in Lagrange formulation, can be found in [1,2], posing no particular problems. Similar Lagrange equations of motion for planar manipulators have been used since many years by numerous authors, let us cite here only [6,7].

Thus, the direct dynamical model is written in Lagrange formulation, as follows [1,2]:

$$\mathbf{A}\ddot{\boldsymbol{\theta}} = \boldsymbol{\Gamma} + \mathbf{b} \tag{1}$$

where $\ddot{\boldsymbol{\theta}} = \begin{bmatrix} \ddot{\theta}_1 & \ddot{\theta}_2 & \ddot{\theta}_3 \end{bmatrix}^T$ is the 3×1 vector of the second time derivatives of the

joint angles/coordinates and $\ddot{\mathbf{\Gamma}} = \left[\ddot{\Gamma}_1 \quad \ddot{\Gamma}_2 \quad \ddot{\Gamma}_3\right]^{\mathrm{T}}$ is the external torques vector. The elements A_{ij} of the 3×3 symmetric matrix **A** depend on angles θ_i (i=1,2,3) as follows [1]:

$$A_{11} = \left(\frac{m_1}{3} + m_2 + m_3\right) l_1^2 + \left(\frac{m_2}{3} + m_3\right) l_2^2 + 2\left(\frac{m_2}{2} + m_3\right) l_1 l_2 \cos\theta_2 +$$
$$+ m_3 l_3 \left[l_1 \cos(\theta_2 + \theta_3) + l_2 \cos\theta_3 + \frac{l_3}{3} \right]$$

$$A_{12} = \left(\frac{m_2}{3} + m_3\right) l_2^2 + \left(\frac{m_2}{2} + m_3\right) l_1 l_2 \cos\theta_2 + m_3 l_3 \left[\frac{1}{2} l_1 \cos(\theta_2 + \theta_3) + l_2 \cos\theta_3 + \frac{l_3}{3} \right],$$

$$A_{13} = m_3 l_3 \left[\frac{1}{2} l_1 \cos(\theta_2 + \theta_3) + \frac{1}{2} l_2 \cos\theta_3 + \frac{l_3}{3} \right];$$

$$A_{21} = A_{12}, \quad A_{22} = \left(\frac{m_2}{3} + m_3\right) l_2^2 + m_3 l_3 \left(l_2 \cos\theta_3 + \frac{l_3}{3} \right), \quad A_{23} = m_3 l_3 \left(\frac{1}{2} l_2 \cos\theta_3 + \frac{l_3}{3} \right);$$

$$A_{31} = A_{13}, \qquad A_{32} = A_{23}, \qquad A_{33} = \frac{m_3 l_3^2}{3}. \tag{2}$$

The components of the 3×1 vector **b** depend on angles θ_i (i=1,2,3) and their derivatives $\dot{\theta}_i$ [1]:

$$b_1 = \left(\frac{m_2}{2} + m_3\right) l_1 l_2 (\sin\theta_2) \dot{\theta}_2 (2\dot{\theta}_1 + \dot{\theta}_2) + \frac{m_3 l_3}{2} \left\{ l_1 [\sin(\theta_2 + \theta_3)] (\dot{\theta}_2 + \dot{\theta}_3)(2\dot{\theta}_1 + \dot{\theta}_2 + \dot{\theta}_3) + \right.$$
$$\left. + l_2 (\sin\theta_3) \dot{\theta}_3 (2\dot{\theta}_1 + 2\dot{\theta}_2 + \dot{\theta}_3) \right\}$$

$$b_2 = -\left(\frac{m_2}{2} + m_3\right) l_1 l_2 (\sin\theta_2) \dot{\theta}_1^2 + \frac{m_3 l_3}{2} \left\{ -l_1 [\sin(\theta_2 + \theta_3)] \dot{\theta}_1^2 + l_2 (\sin\theta_3) \dot{\theta}_3 (2\dot{\theta}_1 + 2\dot{\theta}_2 + \dot{\theta}_3) \right\},$$

$$b_3 = -\frac{m_3 l_3}{2} \left\{ l_1 [\sin(\theta_2 + \theta_3)] \dot{\theta}_1^2 + l_2 (\sin\theta_3) (\dot{\theta}_1 + \dot{\theta}_2)^2 \right\}. \tag{3}$$

The inverse dynamics equations come naturally from the direct dynamics equations (1) in Lagrange formulation [1]:

$$\mathbf{\Gamma} = \mathbf{A}\ddot{\mathbf{\theta}} - \mathbf{b}. \tag{4}$$

So, these inverse dynamics explicit equations provide the external torques inducing the desired motion, described by the evolution of angles θ_i (i=1,2,3). The computation of the external torques using (4) is trivial.

In practice, the evolution of angles θ_i (i =1,2,3) are known. Their derivatives $\dot{\theta}_i$ and $\ddot{\theta}_i$ are easily computed using the finite differences technique:

$$\dot{\theta}_i(t_k) = \frac{\theta_i(t_{k+1}) - \theta_i(t_k)}{\Delta t} \quad \text{for } i = 1,2,3 \quad \text{and} \quad \forall\, k = 0,\ldots, N-1 \tag{5}$$

then

$$\ddot{\theta}_i(t_k) = \frac{\dot{\theta}_i(t_{k+1}) - \dot{\theta}_i(t_k)}{\Delta t} \quad \text{for } i = 1,2,3 \quad \text{and} \quad \forall\, k = 0,\ldots, N-2 \tag{6}$$

where $\Delta t = t_{k+1} - t_k$ stands for the incremental time step and where the intermediate time is $t_k = t_0 + \frac{k}{N}(T_F - t_0)$, with $t_0 = 0$ the initial time and with T_F the final time.

This double finite differences computation is precisely enough for our case study.

All in-house inverse dynamics simulations presented in this paper have been validated by an appropriate SIMULINK/SimMechanics model, which provided identic results [1,2] with the in-house code based on equations (2-6). Moreover, the motion of the planar 3-DOF manipulator has been accurately controlled using a PID controller. The PID controller parameters have been tuned and optimized using an appropriate Genetic Algorithm [2]. SimMechanics has been successfully used by other authors [8] to simulate the motion of robot manipulators, e.g., using a PD control and online gravity compensation.

3. CASE STUDY: REDUCTION OF MECHANICAL WORK FOR THE MANIPULATION TASK IN HORIZONTAL PLANE

The considered planar 3-DOF manipulator shown in Fig.1 has the following inertial and geometric characteristics: masses $m_1 = m_2 = 0.1$ kg = 100 g and $m_3 = 0.05$ kg = 50 g, respectively arm lengths $l_1 = 0.08$ m = 8 cm, $l_2 = 0.07$ m = 7 cm and $l_3 = 0.03$ m = 3 cm.

As already mentioned, the manipulation task of this planar 3-DOF manipulator is to move in the horizontal plane from an initial posture (at $t_0 = 0$) given by: $\theta_1(t_0) = -1.047197$ rad = –60°, $\theta_2(t_0) = 1.745329$ rad = 100° and $\theta_3(t_0) = -0.349066$ rad = –20°, to the required final posture given by: $\theta_1(T_F) = 1.308997$ rad = 75°, $\theta_2(T_F) = 1.047197$ rad = 60° and $\theta_3(T_F) = 0.349066$ rad = 20°. Null initial and final velocities are considered. The manipulation task is performed in 20 seconds, considering thus: $t_0 = 0$, $T_F = 20$ s.

The four aforementioned simple engineering trajectory generation possibilities are applied:

3.1. $a^+\_a^-$ trajectory generation method

The trajectory corresponds to the variation/evolution of each θ_i (i=1,2,3) by means of a constant acceleration a^+_i between $t_0 = 0$ and $t_{1/2} = T_F/2$, followed by a constant deceleration $a^-_i = -a^+_i$ from $t_{1/2} = T_F/2$ to T_F. More precisely, the acceleration and deceleration for each θ_i are given by the following expressions, already used in previous study [9] concerning the "smooth" guidance of a linear electrical actuator with ball screw drive:

$$a_i^+ = \frac{2\left[\theta_i(T_F) - \theta_i(0)\right]}{p(T_F - 0)^2}, \quad a_i^- = -\frac{2\left[\theta_i(T_F) - \theta_i(0)\right]}{(1-p)(T_F - 0)^2} \quad \text{for } i = 1,2,3 \qquad (7)$$

with $p = \frac{t_{1/2} - 0}{T_F - 0} = \frac{(T_F/2) - 0}{T_F - 0} = \frac{1}{2}$.

Fig. 2 shows the evolutions of the joint angles θ_i (i=1,2,3) for this simple technique (denoted briefly by "$a^+\_a^-$") of constant acceleration with a^+_i until $t_{1/2} = T_F/2$, followed by constant deceleration with a^-_i, while Fig. 3 shows the linear angular velocities $\omega_i = \dot{\theta}_i$ corresponding to the θ_i evolutions from Fig. 2. The corresponding angular accelerations are: $a^+_{\theta_1}(0...T_F/2) = 0.0235 = -a^-_{\theta_1}(T_F/2...T_F)$, $a^+_{\theta_2}(0...T_F/2) = -0.0069 = -a^-_{\theta_2}(T_F/2...T_F)$ and $a^+_{\theta_3}(0...T_F/2) = 0.0069 = -a^-_{\theta_3}(0...T_F/2)$.

Fig. 4 presents the three external torques Γ_1, Γ_2 and Γ_3, computed by the inverse dynamics approach detailed in previous section, producing the joint angles evolutions from Fig. 2, obtained using $a^+\_a^-$ technique.

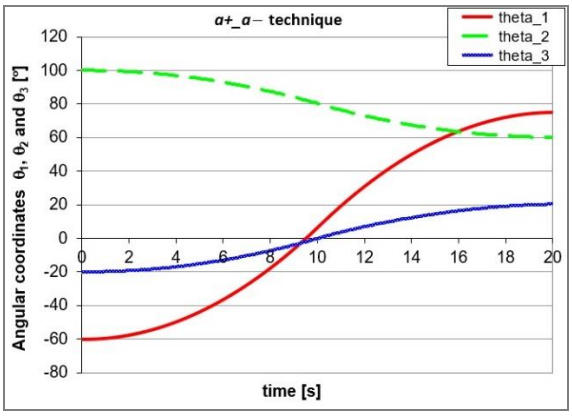

Fig. 2 – Evolutions of the joint coordinates θ_1, θ_2 and θ_3, obtained using the $a^+\_a^-$ technique.

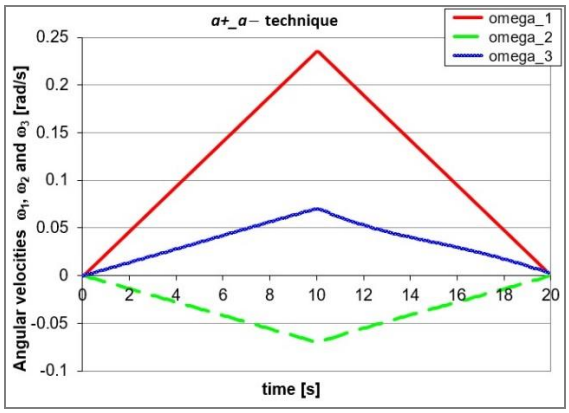

Fig. 3 – Linear angular velocities $\omega_i = \dot{\theta}_i$ for the θ_i angles evolutions from Fig. 2.

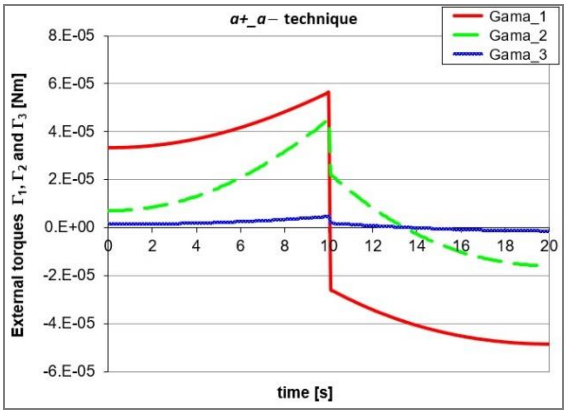

Fig. 4 – Evolutions of the external torques Γ_1, Γ_2 and Γ_3 responsible for the θ_i (i =1,2,3) evolutions from Fig. 2, i.e., for trajectory obtained using the $a^+\_a^-$ technique.

The mechanical works corresponding to the planar 3-DOF manipulator task described by Figs. 2-4 is indicated in Table 1, as follows: $W_1 = 9.74 \cdot 10^{-5}$ Nm (mechanical work of Γ_1), $W_2 = 1.27 \cdot 10^{-5}$ Nm (mechanical work of Γ_2) and $W_3 = 1.34 \cdot 10^{-6}$ Nm (mechanical work of Γ_3). The overall mechanical work is $W = W_1 + W_2 + W_3 = 1.11 \cdot 10^{-4}$ Nm.

3.2. *cos_var* trajectory generation method

The trajectory corresponds to the variation of each θ_i (i =1,2,3) under the form of cosine functions, as follows:

$$\theta_i(t) = \theta_i(0) + \frac{[\theta_i(T_F) - \theta_i(0)]}{2}\left[1 - \cos\left(\frac{\pi t}{(T_F - 0)}\right)\right] \quad \text{for } i = 1,2,3. \tag{8}$$

This second technique concerning θ_i variations is denoted here by "*cos_var*". It can be easily checked that for $t_0 = 0$ expression (7) provides the identity $\theta_i(0) = \theta_i(0)$, while for $t = T_F$ it results the identity $\theta_i(T_F) = \theta_i(T_F)$, finally for $t = t_{1/2} = T_F/2$ expression (7) computes $\theta_i(T_F/2) = \dfrac{\theta_i(0) + \theta_i(T_F)}{2}$.

Fig. 5 shows the cosinusoidal evolutions of the three joint angles θ_i (i =1,2,3) for this second trajectory generation technique called *cos_var*. Fig. 6 shows the angular velocities $\omega_i = \dot{\theta}_i$ corresponding to the θ_i angles evolutions from Fig. 5, while Fig. 7 presents the three external torques Γ_1, Γ_2 and Γ_3, computed by our inverse dynamics approach, inducing the joint angles evolutions from Fig. 5, obtained using *cos_var* technique. The mechanical works and the maximum torques are centralized in Table 1.

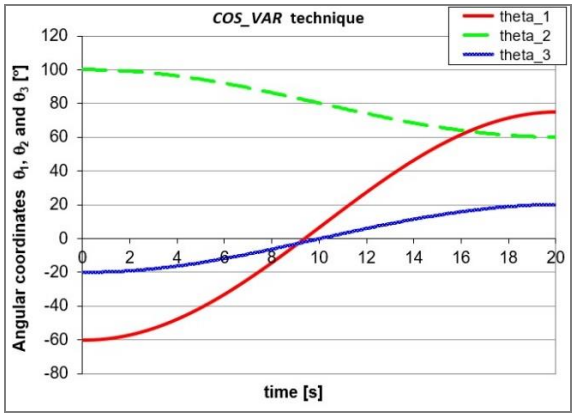

Fig. 5 – Cosinusoidal evolutions of the joint angles θ_1, θ_2 and θ_3 (using *cos_var* technique).

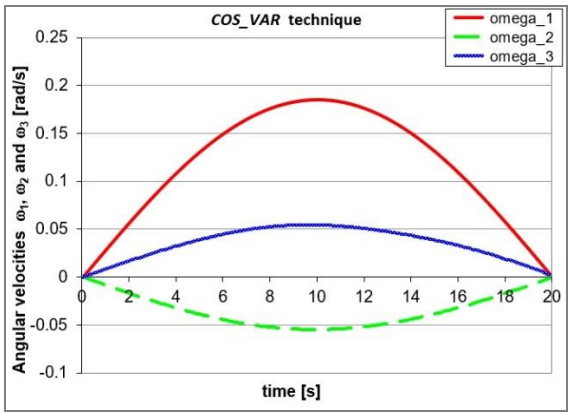

Fig. 6 – Angular velocities $\omega_i = \dot{\theta}_i$ for the θ_i angles evolutions from Fig. 5.

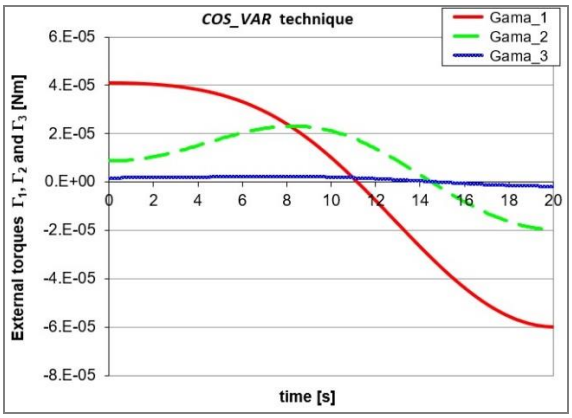

Fig. 7 – Evolution of the external torques Γ_1, Γ_2 and Γ_3 responsible for the *cos_var* cosinusoidal θ_i evolutions from Fig. 5.

3.3. *Linear* trajectory generation method

The trajectory is generated under the form of parameters θ_i (i =1,2,3) showing straight line variations, i.e., linear segments. This third simple trajectory generation method is denoted briefly by "*linear*". A smooth departure at t_0 is considered, with a constant limited acceleration, while at T_F the θ_i variation shows a smooth deceleration.

Fig. 8 shows the *linear* evolutions of the three joint angles θ_i (i =1,2,3) for this third simple technique (the smooth "departures" at t_0 and "arrivals" at T_F are also visible on Fig. 8), while Fig. 9 shows the angular velocities $\omega_i = \dot{\theta}_i$ corresponding to the linear θ_i angles evolutions from Fig. 8.

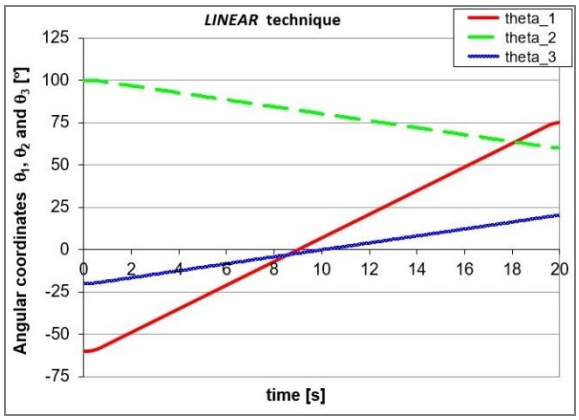

Fig. 8 – Evolution of the joint angles θ_1, θ_2 and θ_3 for the *linear* case, where they vary linearly from θ_i (t_0 =0) to θ_i (T_f =20s).

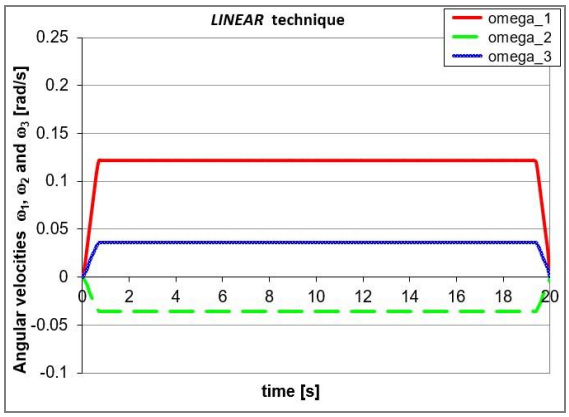

Fig. 9 – Angular velocities $\omega_i = \dot{\theta}_i$ for the *linear* θ_i angles evolutions from Fig. 8.

Fig. 10 shows the three external torques Γ_1, Γ_2 and Γ_3, computed by the proposed inverse dynamics approach, producing the joint angles evolutions from Fig. 8, obtained using this *linear* technique. For a better visualization of the "regular" external torques, Fig. 11 presents a zoomed detail of Fig. 10. So far, as shown in Table 1, the linear evolutions of the θ_i (i =1,2,3) angles correspond to the smallest overall mechanical work, compared with $a^+\_a^-$ and *cos_var* techniques.

Finally, Fig. 12 shows the corresponding manipulator motion.

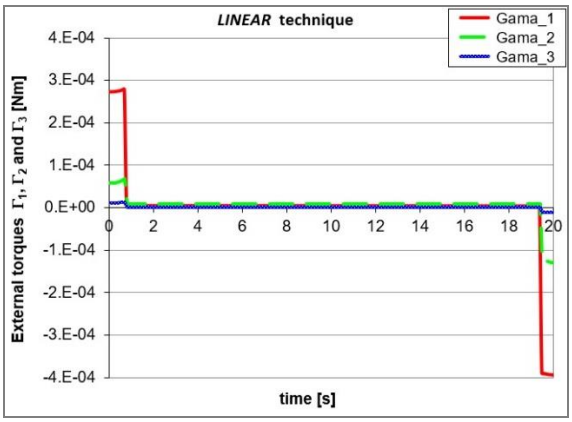

Fig. 10 – Evolution of the external torques Γ_1, Γ_2 and Γ_3 corresponding to the *linear* angles variation from Fig. 8.

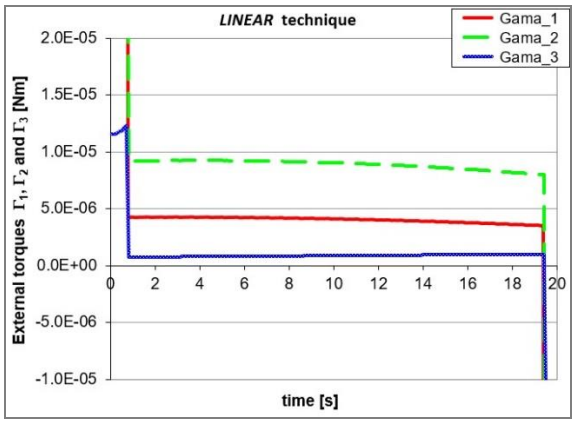

Fig. 11 – Zoomed detail of Fig. 10, showing the external torques Γ_1, Γ_2 and Γ_3 corresponding to the *linear* angles variation from Fig. 8.

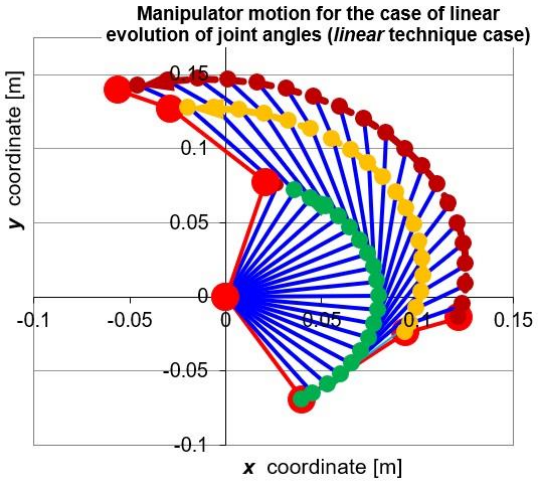

Fig. 12 – Planar 3-DOF manipulator motion for the *linear* evolution of θ_i from Fig. 8.

3.4. *Bilinear* trajectory generation method

For this *bilinear* case, the trajectory is obtained by considering the evolutions of angles $\theta_1(t)$, $\theta_2(t)$ and $\theta_3(t)$ between the initial time $t_0 = 0$ and the final time T_F, as linear segments between $t_0 = 0$ and $t_{1/2} = T_F/2$ on one hand, and other linear segments between $t_{1/2} = T_F/2$ and T_F on the other hand. More precisely, we consider that each θ_i (i =1,2,3) evolves from $\theta_i(t_0)$ to $\theta_i(T_F)$ by means of two simple linear segments, one segment from t_0 to $T_F/2$ and another segment from $T_F/2$ to T_F. This fourth trajectory generation simple method will be denoted shortly as *bilinear*

technique. In this fourth case of *bilinear* trajectory choice, were considered as well smooth departures, arrivals and transitions from one straight line/segment to another one.

In our Matlab/Simulink code, for this *bilinear* technique we have implemented a random allocation of the intermediate values $\theta_1(T_F/2)$, $\theta_2(T_F/2)$ and $\theta_3(T_F/2)$, more precisely:

$$\theta_i\left(\frac{T_F}{2}\right) = \theta_i(0) + \text{rand}_i \cdot \left[\theta_i(T_F) - \theta_i(0)\right] \quad \text{for } i = 1,2,3. \tag{9}$$

where rand_i is a randomly generated number between 0 and 1.

So far, this random allocation of $\theta_1(T_F/2)$, $\theta_2(T_F/2)$ and $\theta_3(T_F/2)$ values has been implemented as a single/manual search in the framework of this *bilinear* technique. But an automatic Matlab code can be easily programmed, testing rapidly hundreds of such single searches based on random allocation of $\theta_i(T_F/2)$. Such an automatic Matlab code would represent a more or less evolved search method. Further studies will also compare this automatic search method with methods like Genetic Algorithm, which can be used to deal with planar redundant manipulators obstacle avoidance and overall joint displacements minimization [4, 5], with the end-effector achieving a number of prescribed configurations.

We have performed around 20 manual searches consisting of random allocations of $\theta_1(T_F/2)$, $\theta_2(T_F/2)$ and $\theta_3(T_F/2)$ values. Fig. 13 shows one of these *bilinear* evolutions of the three joint angles θ_i (i =1,2,3), more precisely the one corresponding to the smallest overall mechanical work (indicated in Table 1). One can remark that in what concerns θ_1, which is the joint angle evolution influencing the most the overall mechanical work, its evolution is almost *linear*. On Fig. 13 are also visible the smooth "departures", "arrivals" and "transitions" from one straight line/segment to another one.

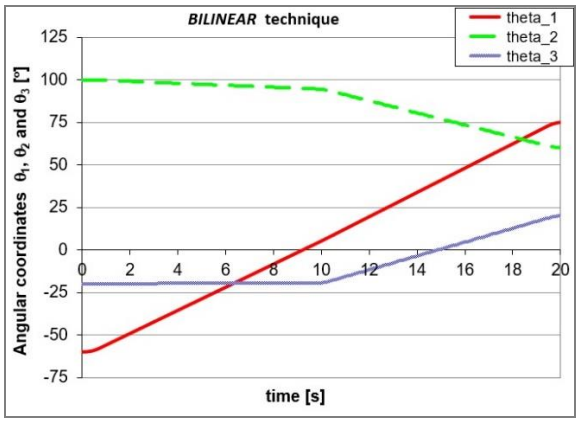

Fig. 13 – Evolution of the joint angles θ_1, θ_2 and θ_3 for the "best" *bilinear* case, corresponding to $\theta_1(T_F/2) = 5.19°$, $\theta_2(T_F/2) = 94.35°$ and $\theta_3(T_F/2) = -19.36°$.

Fig. 14 shows the angular velocities $\omega_i = \dot{\theta}_i$ corresponding to the linear θ_i angles evolutions from Fig. 13.

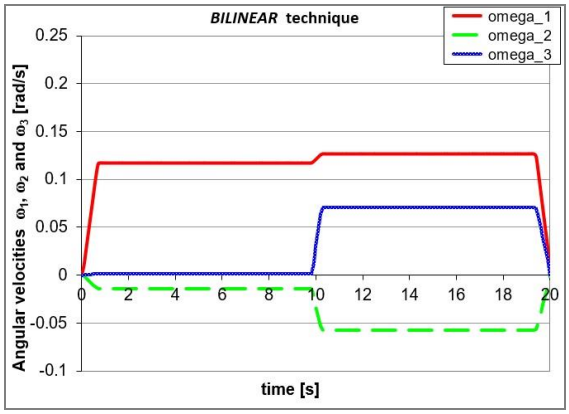

Fig. 14 – Angular velocities $\omega_i = \dot{\theta}_i$ for the *linear* θ_i angles evolutions from Fig. 13.

Fig. 15 shows the three external torques Γ_1, Γ_2 and Γ_3, computed by the inverse dynamics approach, producing the joint angles evolutions from Fig. 13, obtained using *bilinear* technique. Fig. 16 presents a zoomed detail of Fig. 15.

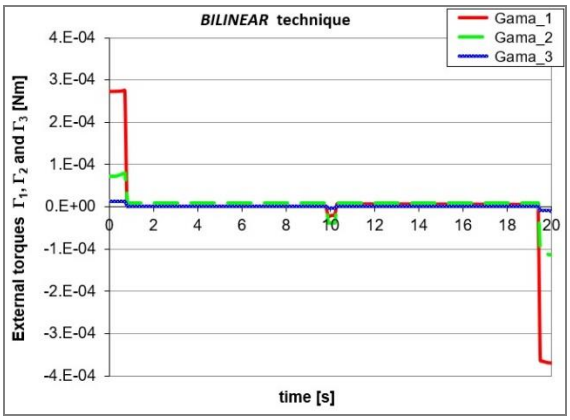

Fig. 15 – Evolution of the external torques Γ_1, Γ_2 and Γ_3 corresponding to the *bilinear* variation of joint angles θ_i from Fig. 13.

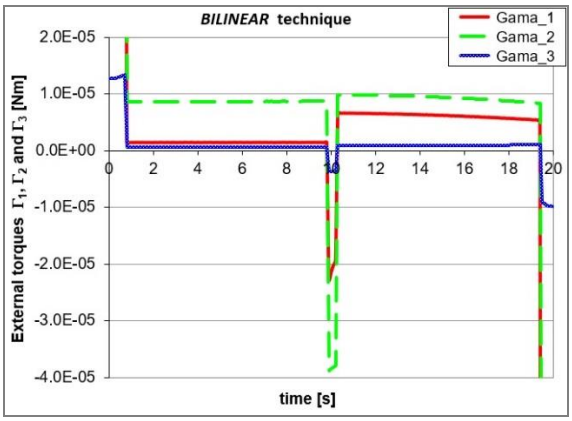

Fig. 16 – Zoomed detail of Fig. 15, showing the external torques Γ_1, Γ_2 and Γ_3 corresponding to the *bilinear* angles variation from Fig. 13.

3.5. Comparison in terms of mechanical works and maximum torques between the 4 simple trajectory generation methods

Table 1 presents the mechanical works and maximum torque values for the four simple methods of trajectory generation proposed above: $a^+\_a^-$, *cos_var*, *linear* and *bilinear*, respectively. Let us recall that the case study here concerns a manipulation task in the horizontal plane, where the planar 3-DOF manipulator moves, in 20 sec, from an initial posture (at $t_0 = 0$) given by: $\theta_1(t_0) = -1.047197$ rad $= -60°$, $\theta_2(t_0) = 1.745329$ rad $= 100°$ and $\theta_3(t_0) = -0.349066$ rad $= -20°$, to the final posture given by: $\theta_1(T_F) = 1.308997$ rad $= 75°$, $\theta_2(T_F) = 1.047197$ rad $= 60°$ and $\theta_3(T_F) = 0.349066$ rad $= 20°$. Null initial and final velocities are considered.

Table 1

Tests performed in order to reduce the overall mechanical work during the manipulation task, using the four simple engineering methods of trajectory generation

technique ID	$W_1(\Gamma_1)$	$W_2(\Gamma_2)$	$W_3(\Gamma_3)$	W(sum)	max(Γ_1)	max(Γ_2)	max(Γ_3)
$a^+\_a^-$	$9.74\cdot10^{-5}$	$1.27\cdot10^{-5}$	$1.34\cdot10^{-6}$	$1.11\cdot10^{-4}$	**$5.67\cdot10^{-5}$**	**$4.56\cdot10^{-5}$**	**$4.74\cdot10^{-6}$**
cos_var	$6.22\cdot10^{-5}$	$1.07\cdot10^{-5}$	$1.13\cdot10^{-6}$	$7.41\cdot10^{-4}$	$5.98\cdot10^{-5}$	$2.32\cdot10^{-5}$	$2.32\cdot10^{-6}$
linear	$3.47\cdot10^{-5}$	$8.14\cdot10^{-6}$	$8.50\cdot10^{-7}$	**$4.37\cdot10^{-5}$**	$3.94\cdot10^{-4}$	$1.30\cdot10^{-4}$	$1.23\cdot10^{-5}$
bilinear	$3.49\cdot10^{-5}$	$9.10\cdot10^{-6}$	$8.77\cdot10^{-7}$	$4.49\cdot10^{-5}$	$3.70\cdot10^{-4}$	$1.14\cdot10^{-4}$	$1.34\cdot10^{-5}$

The information compared between the four trajectory generation methods concerns the mechanical works W_1, W_2 and W_3 produced by Γ_1, Γ_2 and Γ_3 and their sum $W = W_1+W_2+W_3$, as well as the maximum torque values of the three actuators.

The mechanical works and the maximum torque values are expressed in Nm.

In what concerns the smaller overall mechanical work, the best trajectory seems to be the one obtained by the linear variation of θ_i angles (obtained using the *linear* technique), followed very closely by the trajectory obtained using the *bilinear* technique. Further results will show if the *bilinear* technique is able to provide a trajectory involving less overall mechanical work than the *linear* technique trajectory. So far, it seems that the *bilinear* technique trajectory is penalized by the torques needed for the smooth "transition" between the two linear segments in the evolution of each θ_i.

As for the maximum torque values, it seems that the $a^+\_a^-$ technique, followed closely by *cos_var* technique, corresponds to the smaller maximum torque values, being thus the most appropriate for protecting the rotary actuators and thus increasing their lifetime.

4. CONCLUSION AND FUTURE WORK

For the manipulation task from an initial posture to a desired final posture of a planar 3-DOF manipulator in the horizontal plane, this paper proposes simplistic techniques to find solutions/trajectories reducing the overall mechanical work. The protection of the rotary actuators by reducing the maximum torque values is a second criterion considered here. The more appropriate trajectory is searched among the joints angles evolutions obtained using four different simple engineering techniques, denoted briefly by: $a^+\_a^-$, *cos_var*, *linear* and *bilinear*, respectively. The simulations performed so far show that a smaller overall mechanical work corresponds to the trajectories obtained by the *linear* technique (linear evolutions of the three θ_i angles), while the trajectories obtained using the $a^+\_a^-$ and *cos_var* techniques correspond to smaller maximum torque values. Further work will find also the optimal trajectory for this manipulation task and will complete the comparison in terms of mechanical works and maximum torque values. Let us recall that the simplicity is the main advantage of the techniques tested in this paper for manipulation task trajectory generation.

Acknowledgements. This work was supported by a grant of the Romanian Ministry of Research and Innovation, CCCDI – UEFISCDI, project number PN-III-P1-1.2-PCCDI-2017-0086 / contract no. 22 PCCDI /2018, within PNCDI III.

Received on July 8, 2018

REFERENCES

1. DUMITRIU, D., SECARĂ, C, *Dynamics of a planar 3-DOF manipulator*, Proceedings of SISOM 2010 and Session of the Commission of Acoustics, Bucharest, pp. 181−190, May 27-28, 2010.
2. VAN NGUYEN, T., DUMITRIU, D., STROE, I., *Controlling the motion of a planar 3-DOF manipulator using PID controllers*, INCAS Bulletin, **9**, *4*, pp. 91–99, 2017.
3. DUMITRIU, D., ZAHARIA, S.E., VALLÉE, C., *Optimal trajectories generation for robot manipulators using an efficient combination of numerical techniques*, ECCOMAS 2000 Congress, Barcelona, 2000.
4. KAZEM, B.I., MAHDI, A.I., OUDAH, A.T., *Motion planning for a robot arm by using Genetic Algorithm*, Jordan Journal of Mechanical and Industrial Engineering, **2**, *3*, pp. 131−136, 2008.
5. SECARĂ, C., CHIROIU, V., DUMITRIU, D., *Obstacle avoidance by a laboratory model of redundant manipulator using a Genetic Algorithm based strategy*, Proceedings of IV-th National Conference The Academic Days of the Academy of Technical Sciences in Romania, Iassy, Romania, pp. 199−204, 2009.
6. RANKY, P.G., HO, C.Y., *Robot modelling: control and applications with software*, Springer-Verlag, 1985.
7. STOENESCU, E.D., MARGHITU, D.B., *Dynamic effect of prismatic joint inertia on planar kinematic chains*, ASEE Southeastern Section Annual Meeting "Educating Engineering for the Informational Age", Auburn, Alabama, 2004.
8. KANG, H.J., RO, Y.S., *Robot manipulator modeling in Matlab-SimMechanics with PD control and online gravity compensation*, IEEE 2010 International Forum on Strategic Technology IFOST, University of Ulsan, South Korea, pp. 446−449, 2010.
9. DUMITRIU, D., BALDOVIN, D.C., VIDEA, E.M., *Linear motion profile generation using a Danaher Thomson actuator with ball screw drive*, Romanian Journal of Acoustics and Vibration, **11**, *2*, pp. 99−104, 2014.